VIP Electrocatalysis Very Important Paper

DOI: 10.1002/ange.201408408

Scanning Electrochemical Microscopy of Individual Catalytic Nanoparticles**

*Tong Sun, Yun Yu, Brian J. Zacher, and Michael V. Mirkin**

Abstract: *Electrochemistry at individual metal nanoparticles (NPs) can provide new insights into their electrocatalytic behavior. Herein, the electrochemical activity of single AuNPs attached to the catalytically inert carbon surface is mapped by using extremely small (≥3 nm radius) polished nanoelectrodes as tips in the scanning electrochemical microscope (SECM). The use of such small probes resulted in the spatial resolution significantly higher than in previously reported electrochemical images. The currents produced by either rapid electron transfer or the electrocatalytic hydrogen evolution reaction at a single 10 or 20 nm NP were measured and quantitatively analyzed. The developed methodology should be useful for studying the effects of nanoparticle size, geometry, and surface attachment on electrocatalytic activity in real-world application environment.*

Electrochemistry of metal nanoparticles (NPs) has been subject of numerous recent studies because of their extensive applications in electrocatalysis and sensing.[1–3] The catalytic activity of NPs and the reaction pathway often depend strongly on the NP shape, size, and orientation on the surface.[4–6] To investigate the effects of these factors, one has to visualize and measure electrochemical activity at the level of single NPs and crystal-surface facets of a particle. Optical techniques, including surface plasmon resonance imaging,[7] and single-molecule fluorescence imaging[8] were employed recently to map the catalytic activity distribution on a single NP level. One electrochemical approach to single NP experiments is to measure the current at a metal NP either landing at or attached to a small electrode.[9–15] The landing experiments provided more information about transport processes and collision dynamics, the size distribution and concentration of NPs than electron transfer (ET) or catalytic activities. The problems in NP immobilization experiments[13–15] include difficulties in characterizing the geometry of the nanoelectrode/NP system, significant background current produced by the underlying electrode surface, and poorly defined NP shape if it is formed in situ by electrodeposition.

An alternative approach can be more useful for characterization of individual NPs constituting a macroscopic catalyst in real-world application environment. Using a nanoelectrode as a tip in the scanning electrochemical microscope (SECM),[16] one can address an individual NP immobilized on the substrate surface. SECM has previously been employed in studies of electrochemical reactions at surface-immobilized NPs, including heterogeneous ET,[17] the electrocatalytic hydrogen evolution reaction (HER),[18] and oxygen reduction;[6,19] however, no SECM experiments at single immobilized NPs have yet been reported. The Stimming group used a scanning tunneling microscopy (STM) tip to first form a Pd NP by electrodeposition, deposit it onto an Au surface, and then detect H_2 produced by the HER at the NP.[20] One of the difficulties in this pioneering work was that a conical STM tip is not an ideal probe for quantitative electrochemical measurements. In another novel SECM-type experiment, a conductive atomic force microscopy (AFM) tip was used to measure the size and statistical distribution in grafting density of PEG on the NPs modified with a redox-labelled ferrocene/polyethylene glycol capping agent.[21] Scanning electrochemical cell microscopy (SECCM) was used for mapping the electrocatalytic activity of the NP ensemble and showed significant differences in activities of similarly sized NPs.[22]

Here we employ SECM with a disk-type polished Pt tip to image individual AuNPs and probe ET and HERs at their surfaces. Two types of SECM experiments are shown schematically in Figure 1. In a feedback mode experiment (Figure 1 a), a nanometer-sized SECM probe approaches a metal NP, the radius (r_p) of which is either larger than or comparable to that of the tip (a). The electrolyte contains an electroactive mediator (in this work, ferrocenemethanol; Fc) and the tip potential (E_T) is such that the mediator oxidation occurs at a rate governed by diffusion. When the separation distance (d) becomes comparable to a, the oxidized form of

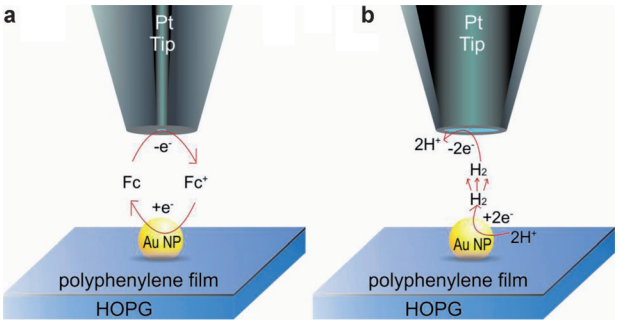

Figure 1. Schematic representation of a) the feedback mode and b) SG/TC SECM experiments at single NPs.

[*] T. Sun, Y. Yu, B. J. Zacher, Prof. M. V. Mirkin
Department of Chemistry and Biochemistry, Queens College of the City University and New York, Flushing, NY 11367 (USA)
E-mail: mmirkin@qc.cuny.edu

[**] The support of this work by the National Science Foundation (grant number CHE-1300158) and AFOSR MURI (< grant number FA9550-14-1-0003) is gratefully acknowledged. We thank Jean-Marc Noël for helpful discussions and Na Lei for her help with the preparation of the figures.

Supporting information for this article is available on the WWW under http://dx.doi.org/10.1002/anie.201408408.

the mediator (Fc^+) produced at the tip surface gets reduced at the substrate, and the tip current increases with decreasing d (positive feedback). The tip current can be recorded as a function of d (approach curve) or tip x–y position (imaging). If no mediator regeneration occurs at the sample, the tip current decreases with decreasing d because of hindered diffusion of redox species (negative feedback). In substrate generation/tip collection mode (SG/TC mode; Figure 1b), d is too long for efficient SECM feedback, and a larger tip ($a > r_p$) collects redox species generated at the NP surface (e.g., H_2 in Figure 1b).

To probe a heterogeneous reaction at the metal NP, it has to be immobilized on a flat, uniform, and electrochemically inert surface that would provide an electrical connection to the particle. Highly ordered pyrolytic graphite (HOPG) can fulfill all these requirements because of its very low roughness, catalytic inertness, and the ease of passivating its surface by the well-established diazonium electrochemistry.[23,24] The subnanometer scale roughness of bare HOPG can be seen in a non-contact mode AFM topography image (Figure 2a) and a feedback mode SECM image of the same HOPG sample (Figure 2b; different areas were imaged by SECM and AFM) obtained with a 33 nm radius polished Pt tip. The electrochemical image shows significant positive feedback (the tip current in the bulk solution, $i_{T,\infty} = 10$ pA) essentially uniform over the entire HOPG surface. SECM approach curves obtained with Fc mediator at a bare HOPG substrate (Figure S2a in the Supporting Information) also showed positive feedback. There are no major spatial variations in the regeneration rate of Fc mediator in the image obtained with a nanometer-sized tip. This observation is in agreement with the finding of the Unwin group that electrochemical reactivity of the graphite basal plane is not significantly lower than that of the step edges.[25]

An AFM image of the compact polyphenylene multilayer assembled on the HOPG surface by electrochemical reduction of the corresponding aryl diazonium salt[24,26] shows subnanometer scale roughness (Figure 2c), only slightly higher than that of bare HOPG (Figure 2a). The corresponding SECM image obtained with a 33 nm tip (Figure 2d) is also featureless with the uniformly negative feedback ($i_{T,\infty} =$ 10 pA). Importantly, the ET across the film appears to be completely blocked, as can be seen from the SECM approach curve in Figure S2b that fits well the theory for pure negative feedback. Although the defect density in polyphenylene films is known to be relatively high, the rate of ET through defects is too slow to produce measurable current at a nanometer-sized tip.

20 nm AuNPs electrostatically attached to the polyphenylene film appear to be about 10-15 nm high and 50 nm in diameter (laterally) in the AFM image (Figure 2e). The height value smaller than the nominal AuNP diameter is expected because the NPs are partially buried in the polyphenylene layer, while a significantly larger lateral NP size in the image is an artifact that has previously been reported and explained by the tip convolution effect.[27] The low particle density on the surface required for electrochemical experiments at individual NPs was attained by immersing the substrate in AuNP solution for 30 minutes.

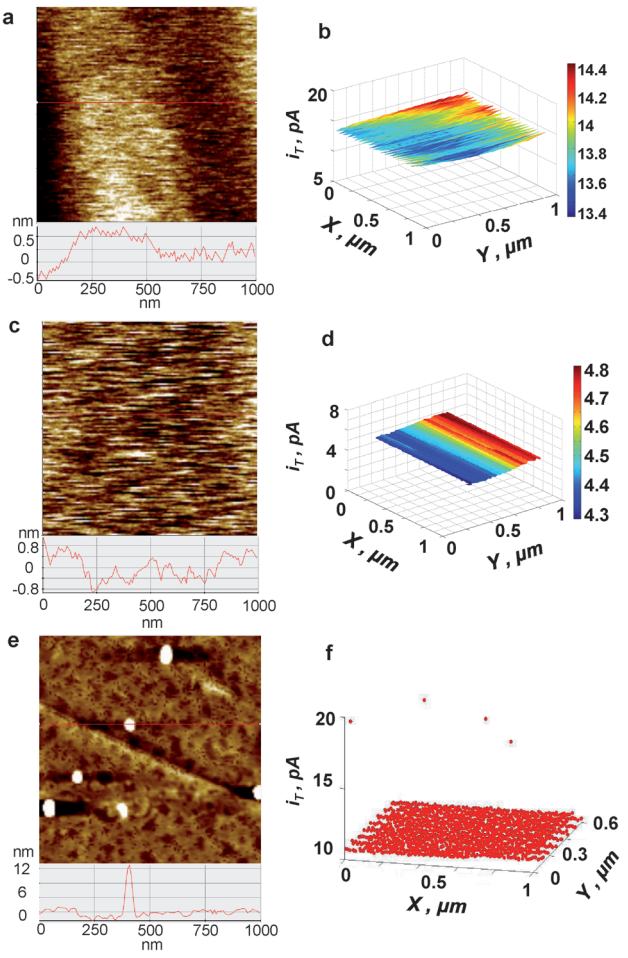

Figure 2. a,c,e) 1×1 µm² non-contact mode topographic AFM and b,d,f) feedback mode SECM images of the bare HOPG surface, HOPG coated with a polyphenylene film, and AuNPs immobilized on the film, respectively. The red lines in (a,c,e) correspond to the shown cross-sections. b,d,f) $E_T = 400$ mV and the substrate was unbiased.

Longer immersion times resulted in a much higher NP density (Figure S3a), and the SECM image of such a substrate showed positive feedback (Figure S3b), suggesting that an ensemble of AuNPs behaved as an unbiased conductive substrate (Figure S4). The NP packing in Figure S3 was too close for individual particles to be seen in the SECM image. In contrast, the SECM image of low density AuNPs (Figure 2f) contains several high spikes of tip current against the much lower background, corresponding to negative feedback over the passivated HOPG surface. These spikes point to the presence of well-separated nanoparticles on the surface, which could not be seen clearly with a relatively large tip ($a = 42$ nm) and low line density (40 nm distance in y axis between the nearest tip scans).

Using a smaller tip (e.g., $a = 14$ nm; Figure 3), one can zoom in on a single AuNP. The 50×50 nm² constant-height SECM image in Figure 3a shows significant positive feedback over the NP surface and negative feedback over the polyphenylene film ($i_{T,\infty} = 4.5$ pA). The NP diameter in Figure 3a is close to the expected 20 nm value, as opposed to 50 nm in the AFM image (Figure 2e). The current–distance curve obtained with the same tip positioned above the same

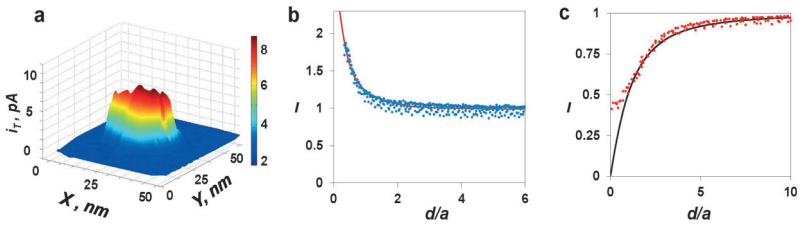

Figure 3. Probing ET at a single 20 nm AuNP by SECM. a) Image of a AuNP on a HOPG/polyphenylene substrate obtained with a 14 nm-radius Pt tip. b,c) Experimental current–distance curves (symbols) and corresponding theoretical curves (solid lines) obtained with the same tip approaching the same AuNP (b) and the insulating portion of the substrate (c; I = normalized current). The solution contained 1 mM Fc and 0.1 M KCl. E_T = 400 mV vs. Ag/AgCl and an unbiased substrate.

NP (symbols in Figure 3b) fits the theory (solid line; see the Supporting Information) very well. The theoretical curve was simulated for a disk-shaped nanoelectrode with $a = 13.6$ nm and RG = 10 (RG = r_g/a, where r_g is the thickness of the insulating glass sheath). The current–distance curve obtained with the same tip over a polyphenylene film fits the theory for the pure negative feedback[28] using RG = 10 and $a = 14.4$ nm (Figure 3c). Importantly, the effective radius values obtained from the best fit in Figures 3b and c are very similar to each other and in good agreement with $a \approx 14$ nm calculated from the diffusion-limiting current of Fc, thus indicating that an electrochemical reaction at a single 20 nm NP can be quantitatively probed by SECM.

The diffusion-controlled positive feedback obtained at an unbiased macroscopic substrate with a low density of immobilized AuNPs points to very efficient ET between the NPs and HOPG surface. In addition to direct electrical connection between the buried AuNPs and HOPG,[26] this behavior may be due to fast ET between the electrode and metal NPs across an insulating film.[29]

Even higher spatial resolution can be attained by using a smaller SECM tip. A constant height image of a 10 nm AuNP in Figure 4a was obtained with a 3 nm-radius polished Pt tip. The correct value of the NP diameter ($\approx$10 nm) indicates that the lateral resolution in this image is significantly higher than that in the AFM images obtained with typical commercial probes. The tip radius (3.1 nm) and the quantitative nature of the SECM experiment with such a small tip were validated by fitting an experimental

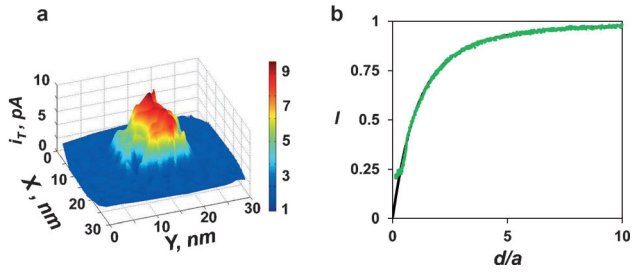

Figure 4. a) 30×30 nm^2 constant-height SECM image of the 10 nm AuNP and b) current–distance curve obtained with the same 3 nm-radius tip approaching the insulating portion of the substrate. The experimental curve (symbols) is fitted to the theory for the pure negative feedback (solid line)[28] with $a = 3.1$ nm (I = normalized current). For other parameters, see Figure 3.

current–distance curve to the theory (Figure 4b). Using similarly sized SECM probes, one may be able to investigate electrochemical processes at specific crystal facets of metal NPs.

Catalytically inert HOPG is a convenient substrate for studying the HER at single AuNPs. The voltammograms in diluted $HClO_4$ solutions (Figure 5a) show no hydrogen evolution waves at either bare HOPG (black curve) or HOPG modified with a polyphenylene film (green curve) at potentials more positive than −900 mV vs. Ag/AgCl reference. A strong catalytic effect of 20 nm AuNPs is seen from the proton reduction wave (red curve).

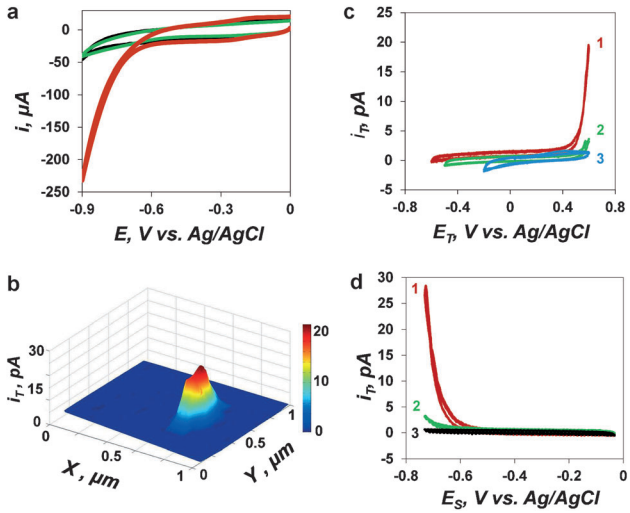

Figure 5. Voltammetry and SECM imaging of the HER at AuNPs. a) Voltammograms of proton reduction at bare HOPG (black), HOPG coated with a polyphenylene film (green), and 20 nm AuNPs immobilized on the modified HOPG (red). b) SG/TC map of the HER at a single 20 nm AuNP obtained with a 15 nm-radius Pt tip. E_T = 500 mV, E_S = −750 mV vs. Ag/AgCl. c) Voltammograms at a 60 nm-radius Pt tip positioned above an AuNP, 80 nm away from the modified HOPG surface. E_T was scanned, and E_S (in mV) was −600 (1), −500 (2), and −100 (3). d) Tip/substrate voltammograms obtained at the same location as in (c). E_S was scanned, and E_T (in mV) was 500 (1), 400 (2), and 100 (3). The solution contained 10 mM $HClO_4$ and 0.1 M $NaClO_4$. The potential sweep rate was $\nu = 100$ mV s^{-1}.

The SG/TC mode image in Figure 5b shows hydrogen flux generated at an AuNP and collected by the 15 nm-radius Pt tip. The tip was positioned 80 nm away from the HOPG/polyphenylene surface and scanned in the x–y plane above the AuNP. The lateral resolution of SG/TC images (and, thus, the apparent size of NPs in Figure 5b) is affected by diffusion broadening.[16] Quantitative information about the HER can be extracted from tip voltammograms obtained at a given E_S value (Figure 5c) and tip/substrate voltammograms (i.e., tip current vs. substrate potential dependences recorded at constant E_T; Figure 5d). Finite-element simulations (see the Supporting Information) showed that 75% of the hydrogen molecules generated at the 10 nm-radius AuNP were reaching the surface of a 60 nm-radius tip under given experimental

conditions. The hydrogen oxidation at the tip occurred at $E_T >$ 400 mV vs. Ag/AgCl (Figure 5c). The wave of hydrogen oxidation was recorded at $E_S = -600$ mV (curve 1), very little hydrogen was detected at $E_S = -500$ mV (curve 2), and essentially no hydrogen at $E_S = -100$ mV (curve 3). Accordingly, the hydrogen oxidation current in Figure 5d is observed when $E_S \leq -500$ mV, and it is negligibly small at $E_T = 100$ mV vs. Ag/AgCl (curve 3), higher at $E_T = 400$ mV (curve 2), and much higher at 500 mV (curve 1).

The collection efficiency in SG/TC mode (i.e., i_T/i_S) is determined by geometry of the tip/substrate system and independent of the substrate potential.[16] Thus, i_T vs. E_S curves in Figure 5d represent the potential dependence of the proton reduction rate at a single AuNP. The linear portion at higher overpotentials of the Tafel plot for this process (Figure 6a; dashed line) obtained from curve 1 in Figure 5d exhibits a 116 mV per decade slope consistent with literature data for HER at polycrystalline gold.[30] The Tafel plot for hydrogen oxidation at the Pt nanoelectrode (Figure 6b) obtained from curve 1 in Figure 5c has the 126 mV per decade slope, which is reasonably close to the 117 mV per decade measured at a polycrystalline Pt microelectrode.[31]

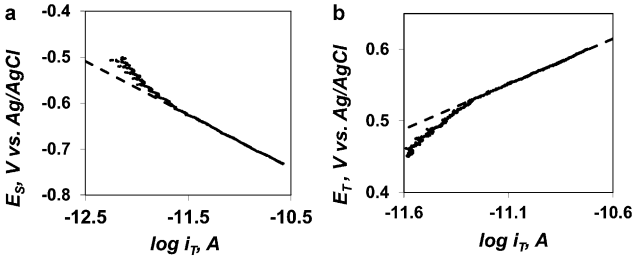

Figure 6. a) Tafel plots for the HER at a single AuNP and b) hydrogen oxidation at the Pt tip.

In summary, unprecedented spatial resolution of electrochemical imaging was achieved in this study by using very small Pt nanoelectrodes as SECM tips. Thus, it was possible to obtain feedback mode topographic images of 10 and 20 nm AuNPs and probe ET occurring at individual NPs. Because of their well-characterized planar geometry, polished Pt tips are suitable for quantitative kinetic experiments.[32] The current–distance curves obtained with the tip radii as small as 3 nm were in good agreement with the SECM theory, suggesting the possibility of spatially resolved, quantitative studies of heterogeneous processes occurring at single NPs and their crystal facets. A larger tip can be used to collect the flux of species generated by electrocatalytic reaction at a NP. In this way, a Tafel plot was obtained for the HER occurring at a single AuNP. The developed approaches should be useful for characterizing the activities of individual NPs constituting real-world macroscopic catalysts.

Received: August 21, 2014
Published online: October 21, 2014

Keywords: electrocatalysis · nanoelectrochemistry · nanoelectrodes · nanoparticles · scanning electrochemical microscopy

[1] R. W. Murray, *Chem. Rev.* **2008**, *108*, 2688 – 2720.
[2] F. P. Zamborini, L. Bao, R. Dasari, *Anal. Chem.* **2012**, *84*, 541 – 576.
[3] S. E. Kleijn, S. C. Lai, M. T. Koper, P. R. Unwin, *Angew. Chem. Int. Ed.* **2014**, *53*, 3558 – 3586; *Angew. Chem.* **2014**, *126*, 3630 – 3660.
[4] K. Yamamoto, T. Imaoka, W.-J. Chun, O. Enoki, H. Katoh, M. Takenaga, A. Sonoi, *Nat. Chem.* **2009**, *1*, 397 – 402.
[5] M. Nesselberger, M. Roefzaad, R. Fayçal Hamou, P. Ulrich Biedermann, F. F. Schweinberger, S. Kunz, K. Schloegl, G. K. H. Wiberg, S. Ashton, U. Heiz, K. J. J. Mayrhofer, M. Arenz, *Nat. Mater.* **2013**, *12*, 919 – 924.
[6] C. M. Sánchez-Sánchez, J. Solla-Gullón, F. J. Vidal-Iglesias, A. Aldaz, V. Montiel, E. Herrero, *J. Am. Chem. Soc.* **2010**, *132*, 5622 – 5624.
[7] X. Shan, I. Diez-Perez, L. Wang, P. Wiktor, Y. Gu, L. Zhang, W. Wang, J. Lu, S. Wang, Q. Gong, J. Li, N. Tao, *Nat. Nanotechnol.* **2012**, *7*, 668 – 672.
[8] X. Zhou, N. M. Andoy, G. Liu, E. Choudhary, K.-S. Han, H. Shen, P. Chen, *Nat. Nanotechnol.* **2012**, *7*, 237 – 241.
[9] X. Xiao, A. J. Bard, *J. Am. Chem. Soc.* **2007**, *129*, 9610 – 9612.
[10] Y.-G. Zhou, N. V. Rees, R. G. Compton, *Angew. Chem. Int. Ed.* **2011**, *50*, 4219 – 4221; *Angew. Chem.* **2011**, *123*, 4305 – 4307.
[11] R. Dasari, D. A. Robinson, K. J. Stevenson, *J. Am. Chem. Soc.* **2013**, *135*, 570 – 573.
[12] Z. Guo, S. J. Percival, B. Zhang, *J. Am. Chem. Soc.* **2014**, *136*, 8879 – 8882.
[13] S. Chen, A. Kucernak, *J. Phys. Chem. B* **2003**, *107*, 8392 – 8402.
[14] Y. Li, J. T. Cox, B. Zhang, *J. Am. Chem. Soc.* **2010**, *132*, 3047 – 3054.
[15] P. Sun, F. Li, C. Yang, T. Sun, I. Kady, B. Hunt, J. Zhuang, *J. Phys. Chem. C* **2013**, *117*, 6120 – 6125.
[16] *Scanning Electrochemical Microscopy*, 2nd ed. (Eds.: A. J. Bard, M. V. Mirkin), CRC, Boca Raton, FL, **2012**.
[17] J. Zhang, R. M. Lahtinen, K. Kontturi, P. R. Unwin, D. J. Schiffrin, *Chem. Commun.* **2001**, 1818 – 1819.
[18] F. Li, I. Ciani, P. Bertoncello, P. R. Unwin, J. Zhao, C. R. Bradbury, D. J. Fermin, *J. Phys. Chem. C* **2008**, *112*, 9686 – 9694.
[19] A. J. Wain, *Electrochim. Acta* **2013**, *92*, 383 – 391.
[20] J. Meier, K. A. Friedrich, U. Stimming, *Faraday Discuss.* **2002**, *121*, 365 – 372.
[21] K. Huang, A. Anne, M. A. Bahri, C. Demaille, *ACS Nano* **2013**, *7*, 4151 – 4163.
[22] S. C. S. Lai, P. V. Dudin, J. V. Macpherson, P. R. Unwin, *J. Am. Chem. Soc.* **2011**, *133*, 10744 – 10747.
[23] F. Anariba, S. H. DuVall, R. L. McCreery, *Anal. Chem.* **2003**, *75*, 3837 – 3844.
[24] D. Bélanger, J. Pinson, *Chem. Soc. Rev.* **2011**, *40*, 3995 – 4048.
[25] S. C. S. Lai, A. N. Patel, K. McKelvey, P. R. Unwin, *Angew. Chem. Int. Ed.* **2012**, *51*, 5405 – 5408; *Angew. Chem.* **2012**, *124*, 5501 – 5504.
[26] J.-M. Noël, D. Zigah, J. Simonet, P. Hapiot, *Langmuir* **2010**, *26*, 7638 – 7643.
[27] J. Zheng, Z. Zhu, H. Chen, Z. Liu, *Langmuir* **2000**, *16*, 4409 – 4412.
[28] M. V. Mirkin, F.-R. F. Fan, A. J. Bard, *J. Electroanal. Chem.* **1992**, *328*, 47 – 62.
[29] J.-N. Chazalviel, P. Allongue, *J. Am. Chem. Soc.* **2011**, *133*, 762 – 764.
[30] J. Perez, E. R. Gonzalez, H. M. Villullas, *J. Phys. Chem. B* **1998**, *102*, 10931 – 10935.
[31] J. F. Zhou, Y. B. Zu, A. J. Bard, *J. Electroanal. Chem.* **2000**, *491*, 22 – 29.
[32] P. Sun, M. V. Mirkin, *Anal. Chem.* **2006**, *78*, 6526 – 6534.

